Electronic Supplementary Material (ESI) for Journal of Materials Chemistry A.

Supporting Information

Growth of Vertically Aligned $Co_3S_4/CoMo_2S_4$ Ultrathin Nanosheets on Reduced Graphene Oxide as High-performance Supercapacitor Electrode

Xijia Yang, [1] Haiming Sun,[1] Ping Zan, Lijun Zhao* and Jianshe Lian*

Key Lab of Automobile Materials, Ministry of Education, College of Materials Scienceand Engineering, Jilin University, Nanling Campus, Changchun, 130025, P.R. China.

E-mail: lijunzhao@jlu.edu.cn；lianjs@jlu.edu.cn;

Fax: +86-431-85095876

Supporting Figures

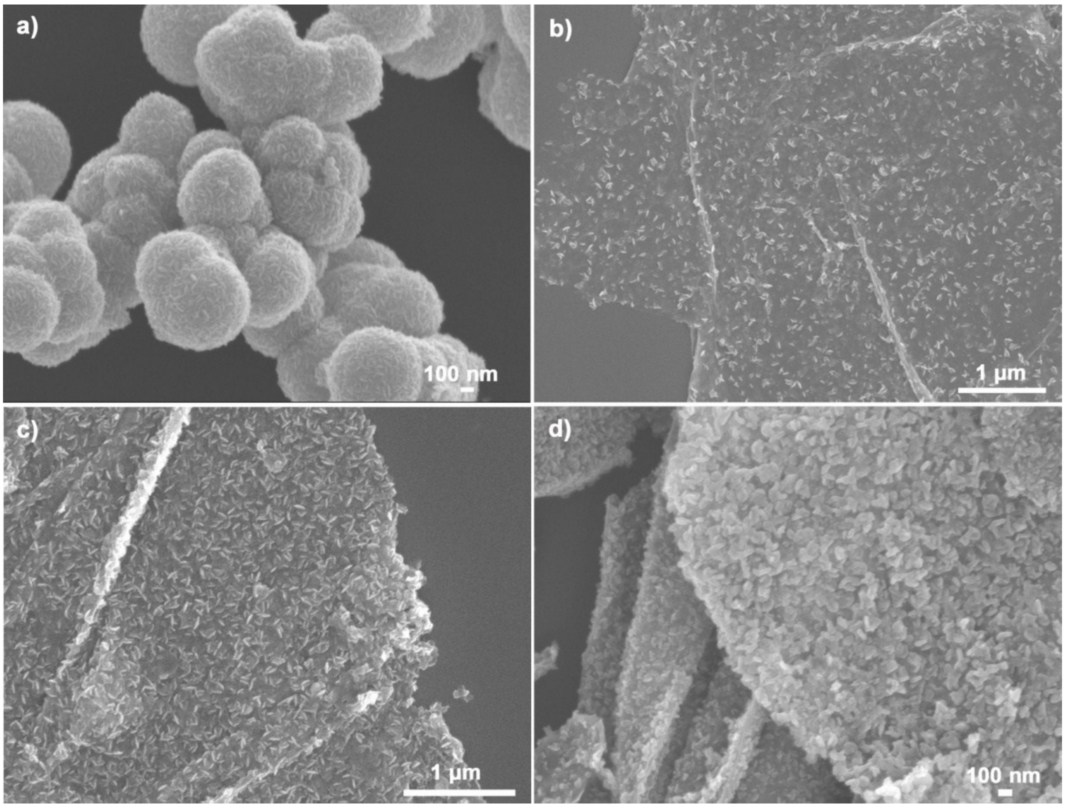

Fig. S1 FE-SEM images of a) the CMS nanoparticles; b) the CMS-rGO hybrid (rGO 15%), c) the CMS-rGO hybrid (rGO 7.5%), d) the CMS-rGO hybrid (rGO 5%).

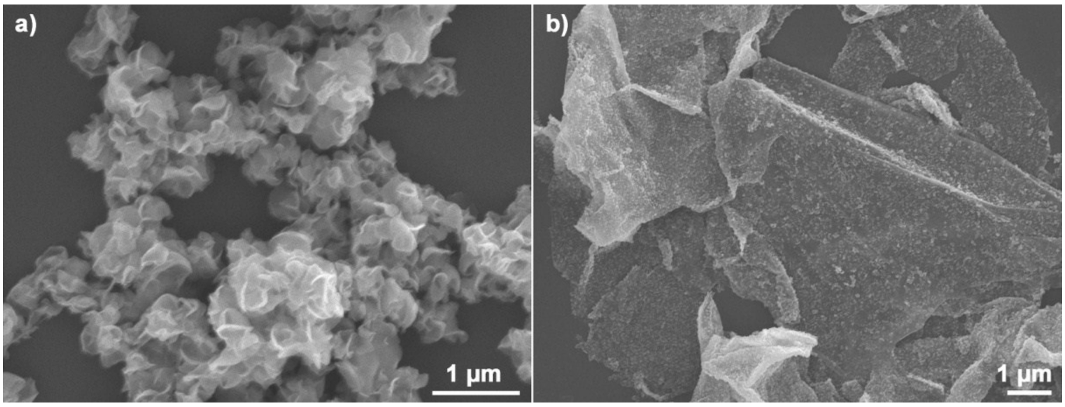

Fig. S2 FE-SEM images of a) the MoS_2-rGO hybrid, b) the Co_3S_4-rGO hybrid.

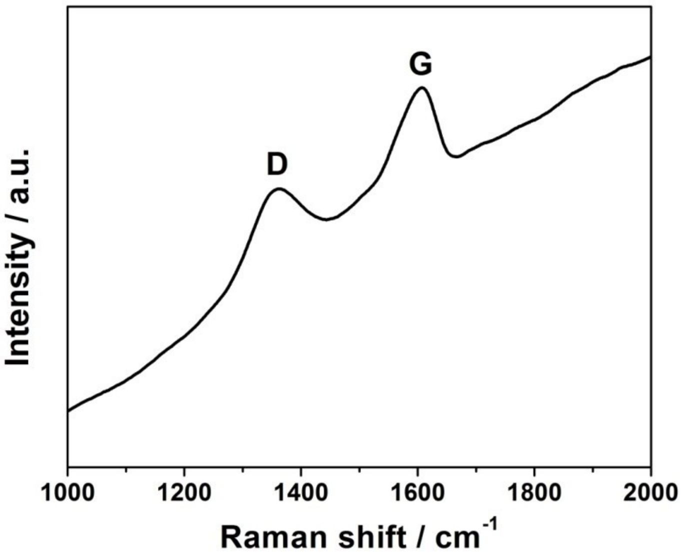

Fig. S3 Raman spectrum of the as-prepared GO.

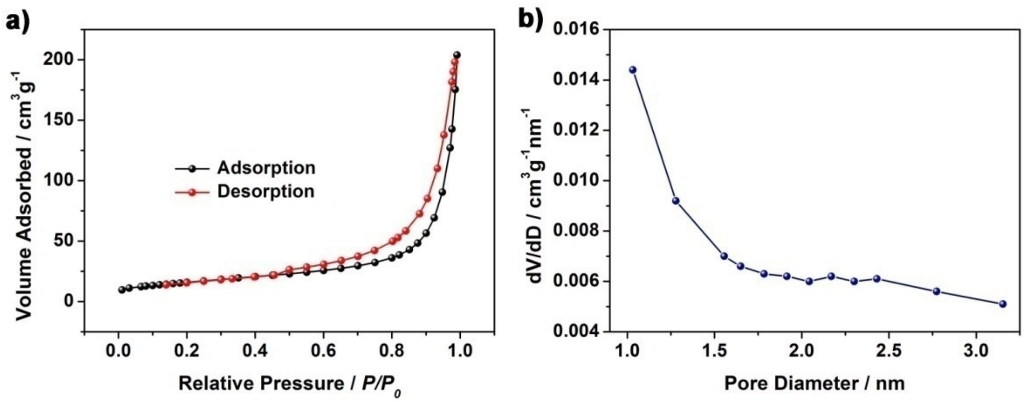

Fig. S4 a) N_2 adsorption–desorption isotherm and b) pore-size distribution curve of the as-obtained CMS-rGO hybrid.

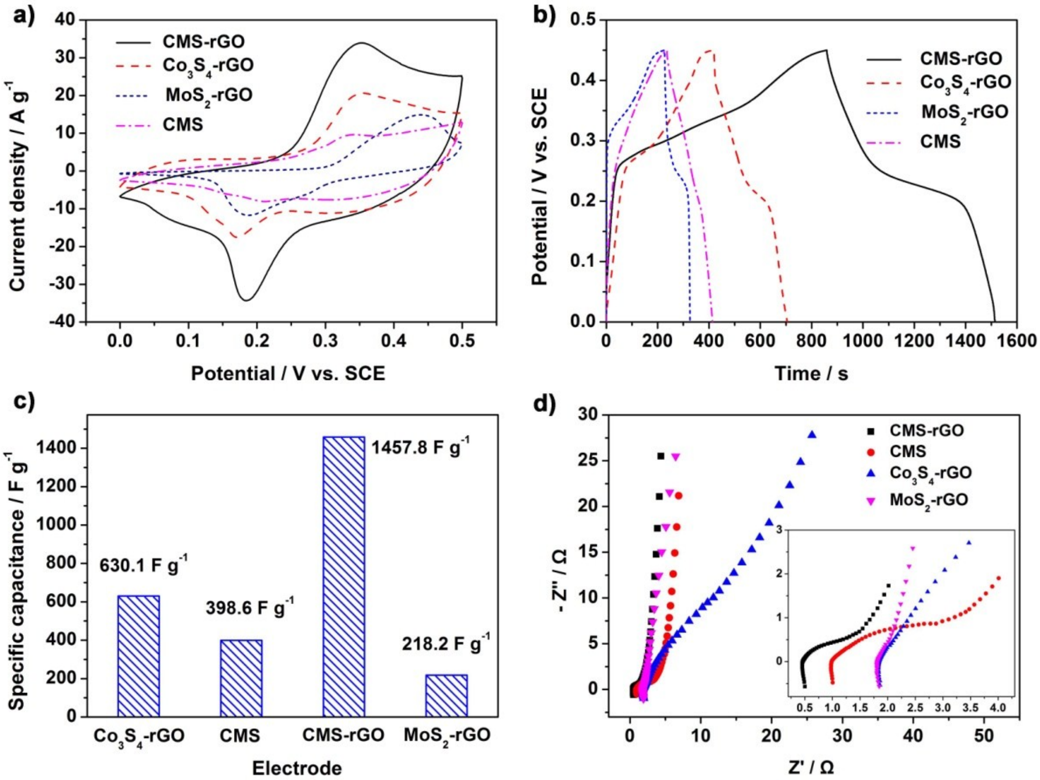

Fig. S5 a) CV curves at the scanning rates of 20 mv s^{-1}; b) charge-discharge curves and c) the calculated specific capacitance of the CMS-rGO, CMS, Co_3S_4-rGO, and MoS_2-rGO electrode. d) Nyquist plots of the CMS-rGO, CMS, Co_3S_4-rGO, MoS_2-rGO electrode.

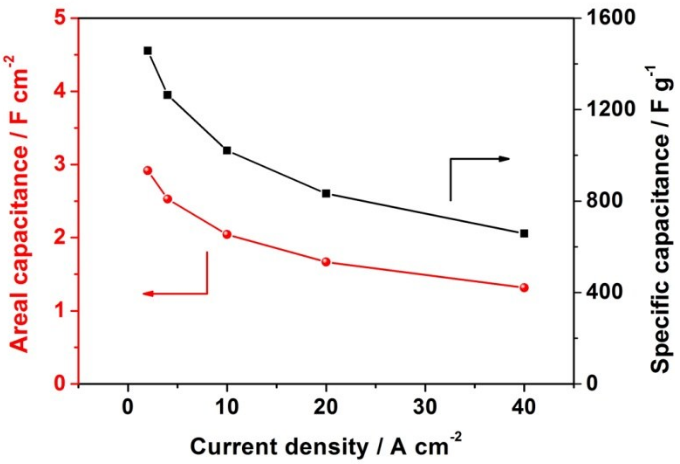

Fig. S6 Specific and areal capacitance of the electrode of CMS-rGO at different current densities.

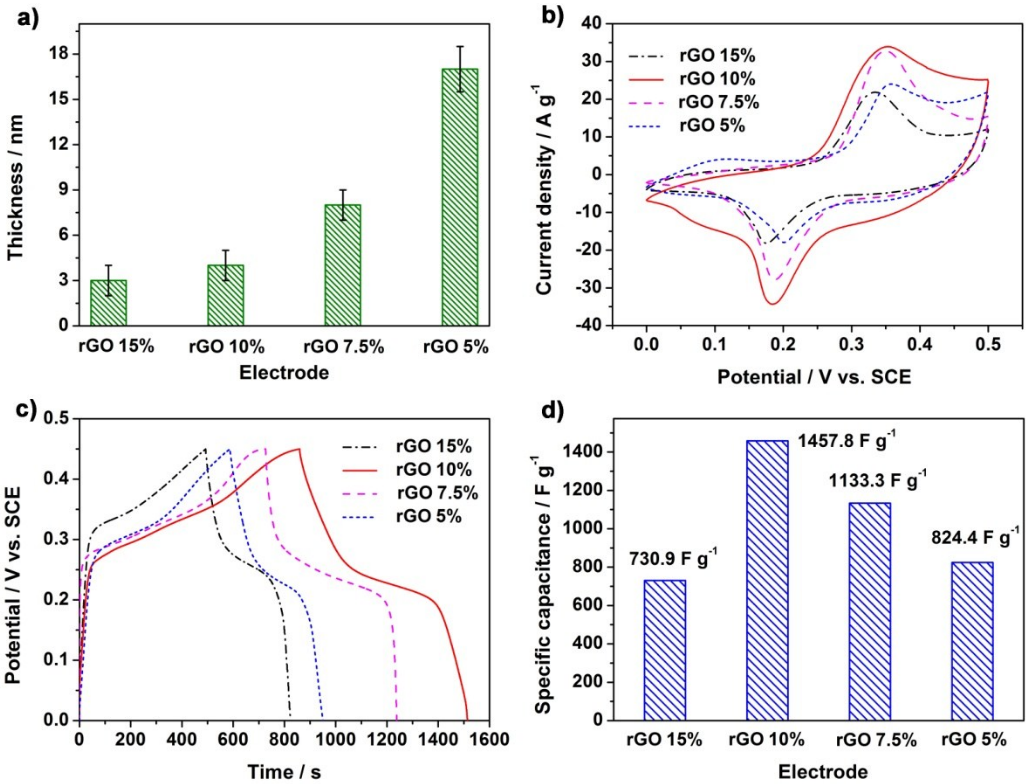

Fig. S7 a) CMS thickness; b) CV curves at the scanning rates of 20 mv s^{-1}; c) charge-discharge curves and d) the calculated specific capacitance of the CMS-rGO (rGO 15%), rGO 10%, rGO 7.5%, and rGO 5% electrode.

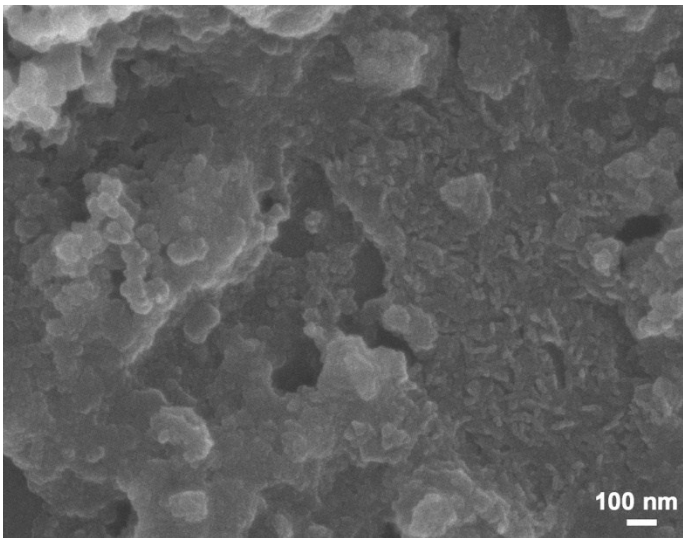

Fig. S8 FE-SEM image of the CMS-rGO hybrid after 2000 cycles.

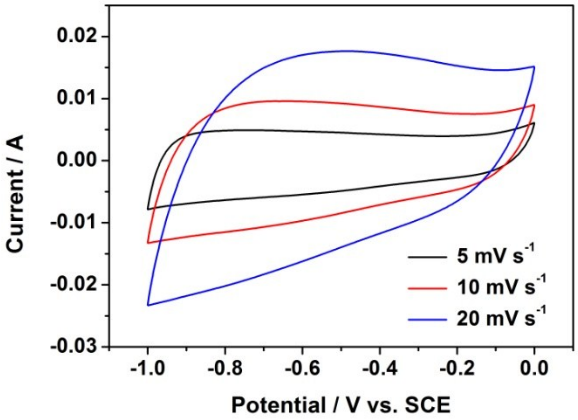

Fig. S9 CV curves AC at the scanning rates of 5 mV s^{-1}, 10 mV s^{-1} and 20 mV s^{-1}.

Table S1 Comparison of the specific capacitance, rate retention, energy density and cycling stability based on Co_3S_4/$CoMo_2S_4$-rGO in present work and other reported work.

Electrode material	Specific capacitance	Rate retention	Energy density	Cycling stability	Reference
Co_3S_4/$CoMo_2S_4$ ultrathin nanosheets on rGO	1457.8 F g^{-1} at 1 A g^{-1}	45.1% 1 to 20 A g^{-1}	33.1 Wh kg^{-1} at 0.85 kW kg^{-1}	93.8% 5000 cycles	This work
Amorphous $CoMoS_4$	661 F g^{-1} at 1 A g^{-1}	62% 1 to 3 A g^{-1}	27.2 Wh kg^{-1} at 0.4 kW kg^{-1}	86% 10000 cycles	1
$NiMoO_4$ nanotubes	864 F g^{-1} at 1 A g^{-1}	70% 1 to 4 A g^{-1}	/	71% 1000 cycles (three-electrode system)	2
MoS_2 nanosheets on N-doped graphene	245 F g^{-1} at 0.25 A g^{-1}	59% 0.25 to 20 A g^{-1}	/	91.3% 1000 cycles (three-electrode system)	3
Porous Co_9S_8 nanostructures on carbon fiber	1056 F g^{-1} at 5 mV s^{-1}	43% 5 to 50 mV s^{-1}	31.4 Wh kg^{-1} at 0.2 kW kg^{-1}	90% 5000 cycles	4
$NiCo_2S_4$@MnO_2 heterostructures	1337.8 F g^{-1} at 2 A g^{-1}	44% 2 to 20 A g^{-1}	/	82% 2000 cycles (three-electrode system)	5
$NiCo_2S_4$@ polypyrrole core−shell heterostructure	9.781 F cm^{-2} at 5 mA cm^{-2}	61.5% 5 to 50 mA cm^{-2}	34.62 Wh kg^{-1} at 0.12 kW kg^{-1}	80.64% 2500 cycles	6
$NiCo_2S_4$ arrays on carbon fiber paper	1154 F g^{-1} at 1 A g^{-1}	62% 1 to 20 A g^{-1}	17.3 Wh kg^{-1} at 0.28 kW kg^{-1}	107% 8000 cycles	7

Notes and references

1 X. Xu, Y. Song, R. Xue, J. Zhou, J. Gao and F. Xing, *Chem. Eng. J.*, 2016, **301**, 266-275.

2 Z. Yin, S. Zhang, Y. Chen, P. Gao, C. Zhu, P. Yang and L. Qi, *J. Mater. Chem. A*, 2015, **3**, 739-745.

3 B. Xie, Y. Chen, M. Yu, T. Sun, L. Lu, T. Xie, Y. Zhang and Y. Wu, *Carbon*, 2016, **99**, 35-42.

4 R. B. Rakhi, N. A. Alhebshi, D. H. Anjum and H. N. Alshareef, *J. Mater. Chem. A*, 2014, **2**,16190-16198.

5 J. Yang, M. Ma, C. Sun, Y. Zhang, W. Huang and X. Dong, *J. Mater. Chem. A*, 2015, **3**, 1258-1264.

6 M. Yan, Y. Yao, J. Wen, L. Long, M. Kong, G. Zhang, X. Liao, G. Yin and Z. Huang, *ACS appl.mater.interfaces*, 2016, **8**, 24525-24535.

7 X. Xiong, G. Waller, D. Ding, D. Chen, B. Rainwater, B. Zhao, Z. Wang and M. Liu, *Nano Energy*, 2015, **16**, 71-80.